Carbohydrate Polymers 198 (2018) 601–610

Contents lists available at ScienceDirect

Carbohydrate Polymers

journal homepage: www.elsevier.com/locate/carbpol

Comparison of soybean hull pre-treatments to obtain cellulose and chemical derivatives: Physical chemistry characterization

Paola Camiscia[a], Enrique D.V. Giordano[a], M. Emilia Brassesco[a], Pablo Fuciños[b], Lorenzo Pastrana[b], M.F. Cerqueira[b,c], Guillermo A. Picó[a,*], Nadia Woitovich Valetti[a]

[a] Instituto de Procesos Biotecnológicos y Químicos (CONICET-UNR), Facultad de Ciencias Bioquímicas y Farmacéuticas, Universidad Nacional de Rosario, Suipacha 570, (2002 RLK), Rosario, Argentina
[b] International Iberian Nanotechnology Laboratory (INL), Avda, Mestre José Veiga s/n, 4715 Braga, Portugal
[c] Centro e Departamento de Física, Universidade do Minho, Campus de Gualtar 4710-057 Braga, Portugal

ARTICLE INFO

Keywords:
Soybean hull
Cellulose
Waste
Bleaching
Thermogravimetry

ABSTRACT

The cellulose from soybean hull, a waste without value from the argentine agriculture, was successfully obtained by using two different treatments: the traditional alkaline-bleaching pathway and from a simple pre-alkaline treatment at low temperatures. The comparison of both methods yielded similar results regarding its ability to open the lignin cellulosic structure of the hull and the total elimination of the lignin content. Fourier Transform Infrared spectroscopy (FT-IR), Thermogravimetric analysis (TGA), Scanning electron microscopy (SEM), ^{13}C nuclear magnetic resonance (^{13}C-RMN) and Raman spectroscopy were used to characterize the structures and the properties of cellulose. The results showed that cellulose can be easily obtained with just an alkaline pre-treatment of 5% (w/v) NaOH during 40 h at 50 °C and free of any lignin content. The attachment of different functional groups, such as -COOH and $(CH_3)_3N^+$, changed the physicochemical properties of the obtained cellulose, showing mayor crystalline structure, and consequently modifying the swelling capacity and its ability to adsorb model proteins.

1. Introduction

Argentina is the third world producer of soybean, with 56 million tons in 2017, where the main products obtained during its processing are proteins and oil to generate biofuel. However, it is being paid little attention to the waste produced from this processing: the soybean hulls, which correspond to about 2% of the total mass. A little part of this waste is used as animal food; however, a great part is burned, or discarded into the environment, producing a negative effect on it. Soybean hulls (SBH) are composed by lignocellulosic material: cellulose (CL) and hemicellulose, which are polysaccharides, and in this case, it has a small proportion of lignin (aromatic polymers resulting from the oxidative combinatorial coupling of 4-hydroxyphenylpropanoids) compared to other biomass waste such as rice hulls, sugarcane bagasse and wheat straw, etc. This biomass waste contains many molecules that have high value and deserve to be isolated and purified for later use in biotechnology (Phinichka & Kaenthong, 2018). Its main component is CL, which has many applications in different branches of biotechnology: food, medicine, bioremediation, paper industry, etc. In terms of biorefinery, the components found in the lignocellulosic biomass can be converted to biopolymers or even to fuels, which have high commercial value.

There are a great number of papers about the treatment of different types of residual biomass (wood, cob, hull, etc.) that opens the rigid lignocellulose structure to favour the liberation of soluble molecules such as pectin and xylan (Carvajal, Gomez, & Cardona, 2016; Karki, Maurer, & Jung, 2011; Kumar & Christopher, 2017). An alkaline pre-treatment has been the most successful delignification method due to its ability to disrupt the ester bonds that are crosslinking lignin and xylan, providing fractions enriched with CL and hemicelluloses (McIntosh & Vancov, 2011). The important modification done by this alkaline pre-treatment (NaOH or KOH) is the disruption of -OH bonding in the fibre

Abbreviations: SBH, soybean hull; CL, cellulose; CLT, functionalized cellulose with tartaric acid; CLC, functionalized cellulose with citric acid; CLA, functionalized cellulose with quaternary ammonium groups

* Corresponding author.
E-mail addresses: camiscia@iprobyq-conicet.gob.ar (P. Camiscia), giordano@iprobyq-conicet.gob.ar (E.D.V. Giordano), brassesco@iprobyq-conicet.gob.ar (M.E. Brassesco), pablo.fucinos@inl.int (P. Fuciños), lorenzo.pastrana@inl.int (L. Pastrana), fatima.cerqueira.vt@inl.int (M.F. Cerqueira), pico@iprobyq-conicet.gob.ar (G.A. Picó), woitovichvaletti@iprobyq-conicet.gob.ar (N. Woitovich Valetti).

https://doi.org/10.1016/j.carbpol.2018.06.125
Received 30 April 2018; Received in revised form 28 June 2018; Accepted 30 June 2018
Available online 02 July 2018
0144-8617/

structure producing ionization and leading to an alkoxide:

$$Fiber{-}OH + NaOH \rightarrow Fiber{-}O^{-}Na^{+}\,(alkoxide) + H_2O$$

That produces the separation of interfibrillar regions of CL fibres. An alkaline treatment of SBH with a low alkali concentration solution (NaOH) removes alkali-soluble substances such as lignin and pectin and other soluble impurities covering the external surface of the fibre cell wall (Andrade-Mahecha, Pelissari, Tapia-Blacido, & Menegalli, 2015; Horn, Vaaje-Kolstad, Westereng, & Eijsink, 2012; Ng et al., 2015). The alkaline pre-treatment changes the chemical structure, the physical structure, dimensions, morphology and mechanical properties of the biomass.

Many authors (Chukwuemeka, Azubuike, Augustine, & Okhamafec, 2012; Ferrer, Salas, & Rojas, 2016; Lu & Hsieh, 2010; Stefanidis et al., 2014) used an alkaline medium (NaOH or KOH) with concentration between 5% (w/v) to 20% (w/v) and temperature that range from 20 °C–120 °C, or instead used sulphuric acid 65% (w/v) at 80 °C–120 °C and were able to solubilize the lignin, xylan and pectin from wood and other biomass. Due to the fact that during the alkaline pre-treatment not all the lignin is lost, a second bleaching process was applied by using chlorinated agents such as $NaClO_2$ or oxidant agents such as H_2O_2 in an alkaline medium and also a temperature range between 20 °C–120 °C (Flauzino Neto, Silvério, Dantas, & Pasquini, 2013). The final product obtained is a mixture of amorphous, fibrillary and crystalline CL. Another method treated SBH (Liu, Wang, & Liu, 2016) with water at temperatures between 130 °C–180 °C to induce the release of saccharides. Other treatment (Martelli-Tosi, Torricillas, Martins, Assis, & Tapia-Blácido, 2016) used four different chemical pre-treatments to obtain CL from SBH: NaOH solution 5% (w/v) or 17.5% (w/v) under two conditions: 90 °C for 1 h, which was repeated twice, followed by 15 h at 30 °C. The fibres were then bleached by using two types of solutions: a solution containing 0.7% (v/v) acetic acid and 3.3% (v/v) $NaClO_2$, agitated at 75 °C for 4 h; and another solution containing H_2O_2 4% (v/v), NaOH 2% (w/v), and $MgSO_4{\cdot}7H_2O$ 0.3% (w/v) (as stabilizer) at 90 °C for 3 h. The fibres were filtered and washed with distilled water until reaching neutral pH, and then washed with ethanol and acetone.

There are few justifications why these experimental conditions were chosen. The disparity in the chemical conditions of these treatments, that induce the opening of the lignocellulosic structure, is a process with high costs on chemical reagents and energy. A mild, non-expensive hydrolysis should be found to make easier the scaling up production of CL.

Here, a simple, different and straightforward route for the use of SBH is proposed to obtain CL and different functional CL from it, to use as potential adsorption beds and apply it for the bioseparation of industrial enzymes, and for the bioremediation of water containing heavy ions.

To obtain this task, the alkaline pre-treatment and the bleaching process using H_2O_2 on the SBH to obtain crude CL were assayed and the yield of both processes were compared. In a second step, the CL obtained from both processes were characterized, using physicochemical methods. In addition, the attachment of -COOH and $(CH_3)_3N^+$ functionalities by esterification and etherification reactions of CL respectively, were assayed and finally, the capacity to adsorb model proteins was studied with the goal, in a future, to use the CL as a cheaper adsorption bed with potential use in the bio-separation of enzymes in a scaling up level.

2. Material and methods

2.1. Materials

Molinos S.A (San Lorenzo - Santa Fe, Argentina) kindly supplied the soybean hulls (SBH). The soybeans (*Glycine max*) cultivated in the Santa Fe Province – Argentine, were harvested in late March 2017. The industrial plant processes soybeans for oil extraction and isolates proteins, and it receives soy grains without chemical or thermal treatments. After mechanical separation, SBH were first grounded using a high-speed rotary cutter and then passed through a 20-mesh sieve (0.8 to 0.4 mm of particle diameter). The total lignin concentration was 0.7% (w/w), estimated using Van-Soest method and calculated in dry weight of SBH (Van Soest, Horvath, McBurney, Jeraci, & Allen, 1983).

2.2. SBH alkaline pre-treatment

Many reports use NaOH solution between 5% (w/v) to 20% (w/v) to induce the opening of lignocellulosic structure. The NaOH 5% (w/v) was selected because it is a low concentration and during all the process, it was determined that the pH remained in a value of 14. The effect of the pre-treatment was studied by evaluating parameters including: residence time and temperature. Briefly, dilute sodium hydroxide at 5% (w/v) was used to pre-treat SBH samples, the ratio biomass/alkaline solution volume was 1/10, which is enough to remain the pH constant around 14. Solid material was washed with distilled water until the pH was 7, dried by ethanol addition and stored at 20 °C. The effect of the temperature (in the range 20 °C–60 °C) and incubation time (0 h–48 h) was analysed.

Besides, many reports suggest that the biomass obtained from the alkaline pre-treatment has residual lignin content. Therefore, a second step, is proposed wherein an alkaline medium (NaOH 2% (w/v)) at temperatures that range 30 °C to 90 °C and in presence of H_2O_2 (4% v/v) which removes the residual cementing material, mainly lignin, in the pre-treated fibres (Flauzino Neto et al., 2013). This process is also known as delignification or bleaching. The H_2O_2 opens the aromatic rings of lignin and makes it partially soluble, decolorizing this material. In this work a comparison of the products obtained from the alkaline and bleaching treatments is performed.

The production of soluble products during both treatments, such as reducing sugar, soluble lignin and xylose from the degradation of xylan (hemicellulose), was detected by using the following methods:

Soluble lignin: measured by reaction with the Folin-Cicalteau method according to previous report (González, Guzmán, Rudyk, Romano, & Molina, 2003; Kirk & Obst, 1988). Data were reported as phenol equivalents.

Xylose: from the degradation of xylan, measured by the phloroglucinol method (Eberts, Sample, Glick, & Ellis, 1979).

Reducing sugar: from the degradation of CL, measured by the DNS method (Marsden, Gray, Nippard, & Quinlan, 1982).

2.3. Surface modification of CL

The following acid and basic chemical groups were attached to the CL structure as following:

2.3.1. Carboxylation of CL

Citric and tartaric acids are derived from natural biological fermentation and could, therefore, be considered as green chemicals. For our advantages the alpha hydroxy acids have the properties to react with its -OH (Marshall, Wartelle, Boler, Johns, & Toles, 1999; Mendoza, 2014). Three grams of CL were mixed for 30 min with 20 ml of 0.6 M citric acid (Marshall et al., 1999). The acid-soaked CL were dried at 50 °C for 2 h. The reaction between acid and CL proceeded on the infused CL at 120 °C for 90 min in a forced-air oven. The functionalized CL was washed with distilled water for the elimination of the unreacted citric acid until the conductance of the medium was very low, the obtained product was called CLC. The same way was assayed with tartaric acid and the final product was called CLT (Mendoza, 2014). Both products were dried at 60 °C during 12 h.

2.3.2. Quaternization reaction of CL

Quaternary ammonium groups were grafted on to CL with the agent, *N*-(3-chloro-2-hydroxypropyl) trimethylammonium chloride, in

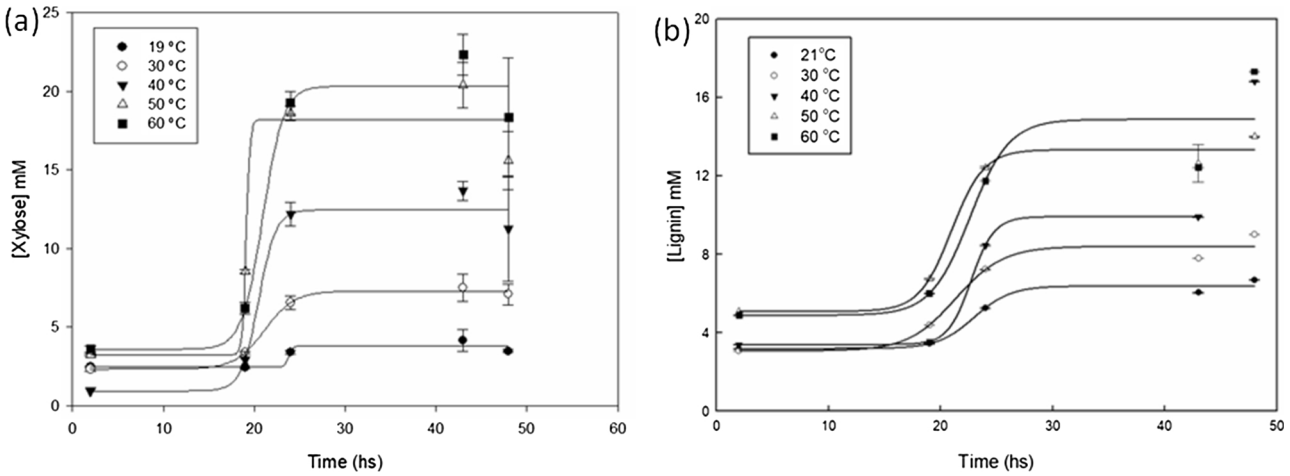

Fig. 1. (a) Kinetics of degradation of xylan vs. time by the alkaline pre-treatment at different temperatures. (b) Lignin degradation expressed as polyphenol production vs. time. Medium NaOH 5% w/v.

an alkaline environment (Prado & Matulewicz, 2014). Three grams of CL were treated with 15 ml of 5 M NaOH for 30 min to provide a basic environment for the quaternizing agent. 15 ml of *N*-(3-chloro-2-hydroxypropyl) trimethylammonium chloride were added to the reaction mixture and CL was incubated at 80 °C for 16 h. The product was then washed with distilled water the same way as before and dried at 60 °C during 12 h. To evaluate the nitrogen content, Kjeldahl method and acid-base titration were used. The obtained compound was called CLA.

2.4. Physical characterization of the CL and functionalized CLs

2.4.1. Swelling analysis

An accurate mass of dried sample was immersed in buffer at 20 °C. At defined time intervals, the materials were withdrawn from the solution and the increase in the weight of the compounds was measured as a function of time until constant mass was achieved. The swelling ratio (SR) is expressed as:

$$SR = \frac{w_2 - w_1}{w_1} \times 100 \quad (1)$$

where: w_1 and w_2 represent the dry and wet weight of the CL and CLs derivates, respectively.

2.4.2. Fourier transform infrared (FT-IR) spectroscopy

IR studies were carried out in a Shimadzu Prestige 21, FT-IR spectrometer, with an attenuated total reflectance (ATR) accessory. The spectra were obtained with 40 scans per spectrum, in the wavenumber range of 4000–700 cm^{-1} with a resolution of 4 cm^{-1}, for each studied sample. The samples were previously frozen at -50 °C and then lyophilized.

2.4.3. ^{13}C NMR spectra in solid state

The spectra of the samples were obtained on a Bruker AC 400/P spectrometer at room temperature. The measurements were gathered at frequencies of 75.47 MHz with a magic angle spinning of 10 kHz. To increase the signal/noise ratio, the CP/ MAS technique was used, with pulse repetition of 5 s and a contact time of 1 ms.

2.4.4. Thermogravimetric analysis (TGA)

Thermogravimetric analysis of CL and functionalized CLs, previously dried at 60 °C during 24 h, was performed on a Gas Controller GC 200, Mettler Toledo Star® System TGA/DSC 1, using 12 mg–20 mg of sample, in the 30 °C – 500 °C interval at a heating temperature rate of 5 °C/min and under argon atmosphere (30 ml/min) to prevent thermo-oxidative degradation. The results were expressed as mass lost in percentage vs. temperature (Yeo, Chin, Tan, & Loh, 2017). The first derivative function was determined by using Sigma Plot v13. A blank without sample was performed.

2.4.5. Determination of the number of acid or basic groups and the $pH_{Z=0}$ value

2 g of CL or functionalized CLs in 20 ml of water was titrated with increasing amount of HCl or NaOH 0.1 M with constant stirring, and then the pH was recorded. The amount of H^+ released or bound per unit of sample mass was calculated. The blank titrations (without the sample) were also carried out. The amount of H^+ or OH^- adsorbed at the final pH were calculated from the amount of the HCl or NaOH added to the samples minus the amount of acid or base used in the blank titration. The pH at zero electrical charge point ($pH_{z=0}$) value for CL and the functionalized CLs were determined (Salis et al., 2011) by mixing 0.5 g of sample and 12.5 ml KCl 25 mM in different reaction vessels. The pH of the suspension was then adjusted to different initial pH values between 2 to 9, using either 0.1 N HCl or NaOH solutions. Each system was agitated in an orbital shaker for 24 h. After settling, the final pH of each suspension was measured. The ΔpH (the difference between final and initial pH) values were then plotted against the initial pH values. The pH at which ΔpH is zero was taken to be the $pH_{Z=0}$.

2.4.6. Scanning electron microscopy (SEM)

The morphology of CL and the functionalized CLs were evaluated by SEM on a Quanta 200 FGE microscope. Samples were coated with a 1–10 nm thick carbon layer and then observed with an accelerating voltage of 3.0 kV.

2.4.7. Raman spectroscopy measurements

These measurements were carried out on an ALPHA300 R Confocal Raman Microscope (WITec) using 633 nm laser for excitation in back scattering geometry. The laser beam with P = 10 mW was focused on the sample by a x50 lens (Zeiss), and the spectra were collected with 600 groove/mm grating using 40 acquisitions with 2 s acquisition time.

3. Results

3.1. Alkaline pre-treatment of SBH

Fig. 1a–b shows the kinetics rate of xylose and lignin liberation from SBH in aqueous medium (expressed as an increase in xylose and polyphenol concentration respectively) where temperature ranges from 20 °C–60 °C. During the liberation of these polymers, a sigmoidal behaviour can be observed with an inflection point around 17–22 h.

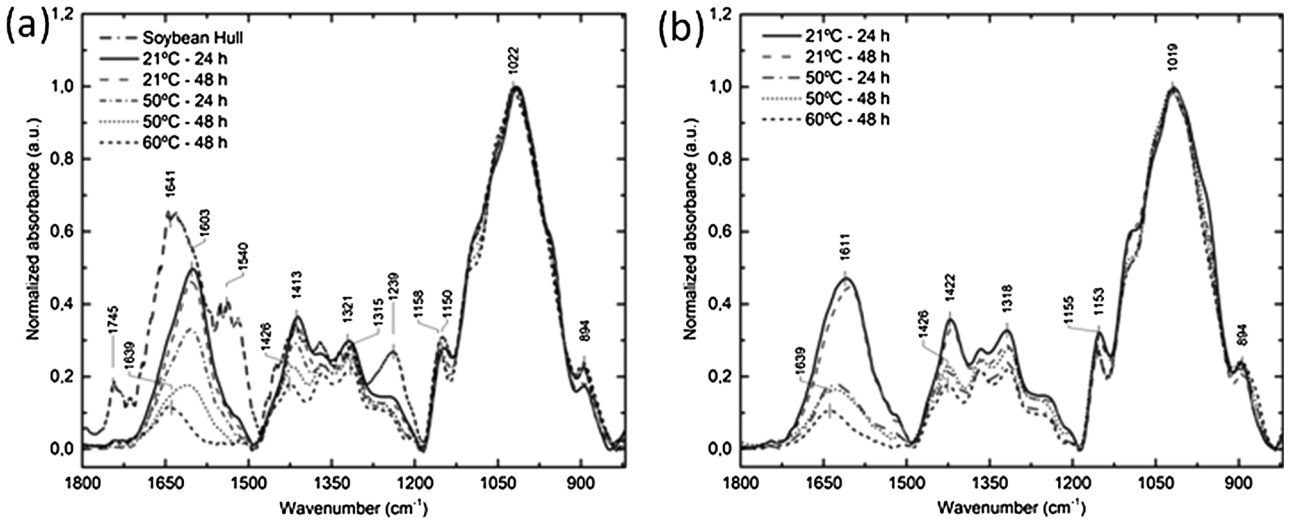

Fig. 2. (a) FT-IR spectra of the SHB alkaline pre-treated at different temperatures and times. Medium NaOH 5% (v/v). (b) FT-IR spectra of the SHB bleaching treatment at different temperatures and times. H_2O_2 concentration 2% (v/v) – NaOH 5% (v/v).

Interesting to note that the time needed to reach the inflection point (around 16–17 h) is approximately the same for temperatures between 20 °C and 40 °C. The liberation of xylose and polyphenol is more evident with the increase of the temperature, indeed at 50 °C and 60 °C there is a significant increase in the liberation of the degradation products, which is congruent with the opening of the ordered structure of the SBH that induces a significant delivery of xylan and lignin. Both plots/curves show a plateau after 30 h. The process was also followed by measuring the soluble reducing sugars in the medium and similar results were observed (data not shown). When using SBH with a particle size of 40 mesh, the results showed no difference (data not shown). The residual biomass was washed many times with distilled water until pH reached 7.0, then dried at 60 °C, lyophilized and stored at room temperature.

3.2. FT-IR of celluloses

Fig. 2a shows the infrared absorbance for a series of alkali pre-treatment done to SBH samples under different conditions of time and temperature and a SBH spectrum without any treatment used as control. The FT-IR spectra shown were normalized to the intensity of the mode that appears at 1020 cm^{-1}, only to better follow the changes that occur during the pre-treatment process. The prominent band in the spectrum at the region of 1200-950 cm^{-1} is related to the C—O, C—C stretching or C—H rock vibrations of CL (Flauzino Neto et al., 2013; Tsuboi, 1957; Xiao, Sun, & Sun, 2001). The region of 1500-1250 cm^{-1} is attributed to $-CH_2$ symmetric bending and CH_2 wagging, and C—OH bending in plane at C-6. The peaks at 1158 cm^{-1} and 894 cm^{-1} are assigned as C—O—C asymmetrical stretching and C—O—C stretching at the β-(1–4)-glycosidic linkage, respectively (Oh et al., 2005). It should be highlighted that in the 1500-1250 cm^{-1} region one should expect bands attributed to the presence of residual hemicelluloses and lignin, such as the S ring (syringyl ring) and G ring (guaiacyl ring) (Pandey, 1999), but they might be masked by the bands of the CL that appear in this same region.

As it was expected, the intensity of the broad peak at 1603 cm^{-1} is markedly reduced as time and temperature increases in the different experimental conditions, owing to the delignification process occurred during the alkaline pre-treatment. The broad peak at 1603 cm^{-1} in the spectra is assigned to aromatic skeletal vibration and C=O stretching, corresponding to the lignin content. In fact, after heating up to 60 °C during 48 h, a small broad peak at 1639 cm^{-1} comes into sight. Moreover, this peak was masked due to the broad peak of lignin, and it is assigned to the bending mode of the absorbed water in the matrix. Under milder conditions of 30–40 h at a temperature of 40–60 °C, the alkaline pre-treatment is sufficiently efficient to hydrolyse the hemicellulose. This is confirmed by the absence of the peak at 1745 cm^{-1}, which is related to either the acetyl and uronic ester groups of the hemicelluloses or the ester linkage of carboxylic group of the ferulic and *p*-coumeric acids of lignin and/or hemicellulose (Sun, Xu, Sun, Fowler, & Baird, 2005). This peak completely disappeared in the treated SBH when the treatment time and temperature where increased, mainly due to the removal of most of the lignin and hemicellulose from the SBH.

Previous reports (Chen, Zhu, Baez, Kitin, & Elder, 2016; Trache et al., 2016) demonstrated an alkali treatment that effectively dissolves hemicellulose, but an extra process was necessary to hydrolyse lignin. In the bleaching method, a chemical oxidant is used, such as $NaClO_2$ or H_2O_2. The bleaching process was performed using H_2O_2 because it can be discarded more easily in the environment afterwards. According to previous reports, different experimental conditions have been assayed to solubilize lignin (Flauzino Neto et al., 2013; Lu & Hsieh, 2010). The chosen condition was 4% (v/v) of H_2O_2 in a medium of NaOH 2% (w/v) at different time and temperature intervals between 0 h and 48 h, and 21 °C and 50 °C, respectively. These conditions were studied in order to determine a milder experimental condition, and were carried out considering the same parameters as the alkaline pre-treatment, as shown in Fig. 2b. Slight changes can be seen when compared to the FT-IR spectra in both processes. In comparison with Fig. 2a, the peak at 1603 cm^{-1} is slightly shifted to higher wavenumbers (1611 cm^{-1}) in the oxidation process. In addition, the band is a bit wider than the alkaline pre-treatment possibly due to oxidation reactions during the bleaching treatment. However, there was not a significant difference between the products obtained from the alkali pre-treatment and the bleaching process. These results shows that hemicellulose and lignin content present in SBH can be extracted by a single treatment in an alkaline medium at 50 °C for 48 h. This pre-treatment permits to avoid the traditionally bleaching with H_2O_2 saving the technical difficulties that can result from the work environment change and the reagent expense.

The SBH composition analysis used in this report, derived from the Argentine Pampa, shows a low lignin concentration of 0.7% (w/w). As it is known, the role of lignin in wood is to make it a very strong material, and the low lignin content in this waste is an advantage for obtaining pure CL by just using mild chemical conditions. So, the elimination of the lignin and the opening of the CL chains can be made under mild conditions, in comparison to other biomass waster such as wood, rise hull, etc. The presence of high lignin content and a closed structure would make it necessary for a more drastic chemical

Table 1
Physical parameters obtained from the cellulose and experimental data from TGA (Tm and residual mass from the pyrolysis) measurements.

System	% water adsorption	ΔpH z = 0	-COOH or $(CH_3)_3N^+$ (meq/g)	T_m TGA (°C)	Residual mass (%)
CL alkaline pretreatment	217.0	9.2	0.44	345	23.8
CLC	57.0	≈ 2.5	3.84	326	20.1
CLA	480.6	3.9	2.3	250 325	22.9
CLT	122.0	≈ 2.5	3.21	342 - 292	10.3

treatment such as using sulfuric acid, and high temperatures. Finally, the CL recovery of the alkaline pre-treatment for 20 preparations was 40.5 ± 6.1% ((41 ± 6) %) of the initial biomass weight.

3.3. Physicochemical characterization of the functionalized CL

Table 1 shows the swelling capacity, $pH_{z=0}$ and the number of acid or basic groups covalent attached per unit mass of sample for CL and functionalized CLs.

3.3.1. Swelling

CL showed a high-water adsorption capacity, which can be attributed to its open structure due to the chemical and thermal treatment. However, the functionalized CLC and CLT showed a significant decrease in their swelling capacity due to crosslinking between the polysaccharides chains and the reagent, induced by reactive alpha hydroxyl acids. Quaternary Ammonium groups were grafted on CLs surface via reaction with *N*-(3-chloro-2-hydroxypropyl) trimethylammonium chloride. In this case it did not induce a crosslinking with the polysaccharide chains of CL because it only reacts with the -OH, so this product opens the three-dimensional structure of the CL which increases the swelling capacity, compared to the CL, CLC and CLT.

3.3.2. Acid base titration and $pH_{Z=0}$

The acid base titration of the CL showed to have 0.44 meq/g, a slightly amount of −COOH acid compared to the other samples, possibly due to pectin. The CLC showed a great number of −COOH meq per unit mass with a value of 3.84 meq/g, while the CLT has 3.21 meq/g, and CLA yielded a 2.3 meq/g of $(CH_3)_3N^+$. Fig. 3 shows the curves that determine $pH_{z=0}$ value for unmodified CL and functionalized CL. Table 1 shows the $pH_{z=0}$ values calculated from the curves.

Below the $pH_{z=0}$ value, the solid material has a positive surface charge, promoting the adsorption of anions, whereas for the pH values above the $pH_{z=0}$ the surface is negatively charged, favouring adsorption of cations (Fiol & Villaescusa, 2009). CL has a high $pH_{z=0}$ value, near 9, which suggests a high anion adsorption, while the CLT and CLC curves intersects the zero point at a very low pH value, near 2, which suggests that their surfaces are always negatively charged. CLA showed a different behaviour and a $pH_{z=0}$ value around 3.90.

3.3.3. SEM: morphological investigation of CL and functionalized CL

Fig. 4A shows a SEM image in which the typical morphology of native CL with its fibrillary structure is visible, in concordance with previous reports (Trache, Donnot, Khimeche, Benelmir, & Brosse, 2014; Ahuja, Kaushik, & Singh, 2018; Trache, Donnot, Khimeche, Benelmir, & Brosse, 2014a,b). The reaction with polyhydroxyl carboxylic acids such as citric and tartaric, induced a narrower and a more compact fibrillary structure as consequence of a decrease in the distance between the fibres, as shown in Fig. 4B and C, due to the crosslinking between the fibres produced by the chemical reaction between the polysaccharide chains and the reagents. Previous works (Zhu, Fan, & Zhang, 2008)

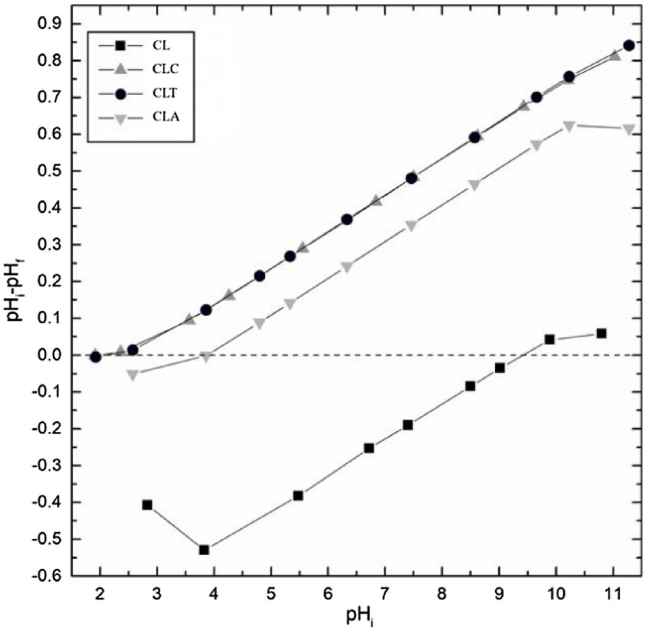

Fig. 3. The ΔpH vs. pH curves for cellulose and functionalized CL, the value that intersects the zero point correspond to the $pH_{z=0}$ of the adsorbent. Medium 20 Mm KCl, temperature: 25 °C.

have studied the reaction of citric acid with polysaccharides chains and observed the formation of two esters bonds between one acid molecule and two carboxylic groups, which induced a crosslinking with the polysaccharides chains and results in a compact structure. Citric acid has three acid carboxylic groups, but only the two external ones can react with the -OH groups of the polysaccharides chains. As a matter of fact, when CL reacts with tartaric acid, which presents two carboxylic acid groups, only one group can produce crosslinking with polysaccharides chains. This can explain the obtained SEM images. Besides, it is consistent with the obtained swelling capacities for these samples.

Fig. 4D shows the morphological aspect of the CLA, in which is seen that the cellulosic fibres are more separated compared to the CL, and the system looks more homogeneous because the reaction conditions requires an alkaline pre-treatment with 20% (w/v) NaOH. Fig. 4E shows the SEM of the CL treated with 20% (w/v) NaOH, where a significant modification of the fibres is observed; this process induced the loss of CL microfibers, resulting in a much less compact structure. The morphological structure of the functionalized CL agrees with their ability of absorb water. CLC and CLT, due to their compact structure, show a very poor swelling capacity in comparison with CL, while CLA has a higher capacity of absorbing water, due to its open structure.

3.3.4. Solid-state ^{13}C NMR spectra of CL and functionalized CL

From the ^{13}C NMR spectra of unmodified CL shown in Fig. 5a it is seen the following chemical shift: the down-field part of the spectrum, the 103–108 ppm region, is assigned to C-1 (anomeric carbon), due to the deshielding effect produced by the oxygen atoms next to that specific carbon. The oxygen from the pyranose ring, O-1 and O-2, has the highest influence, while the O-6 (attached to C-6) has the smallest influence (Kim, Lee, & Kafle, 2013). The others peaks are assigned to C-4 (in the range between 81 and 93 ppm), to C-2, C-3, and C-5 (in the range between 70 and 81 ppm) and finally the peaks between 60 and 70 ppm are assigned to C-6 of the primary alcohol group (Atalla & VanderHart, 1999).

Fig. 5b and c shows the ^{13}C NMR spectra of the esterification reaction by citric and tartaric acid with CL, respectively. In comparison with the pre-treated CL, the spectra displayed a new peak at the region of 168–178 ppm accordingly to the presence of carboxylic acids groups due to the esterification reaction. In addition, there is a slightly overlap

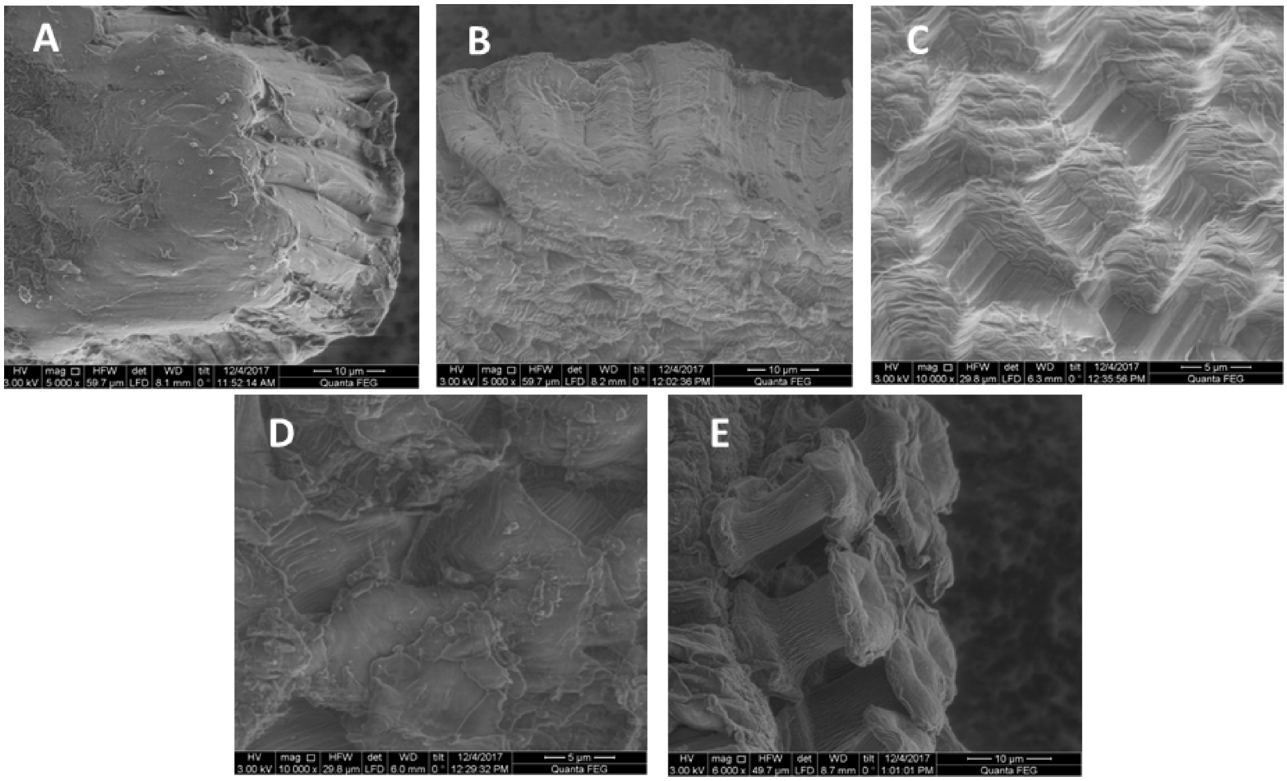

Fig. 4. Electronic micrographs of: A) CL, B) CLC, C) CLT, D) CLA and E) pre-treatment with NaOH 20% (w/v) at 20 °C.

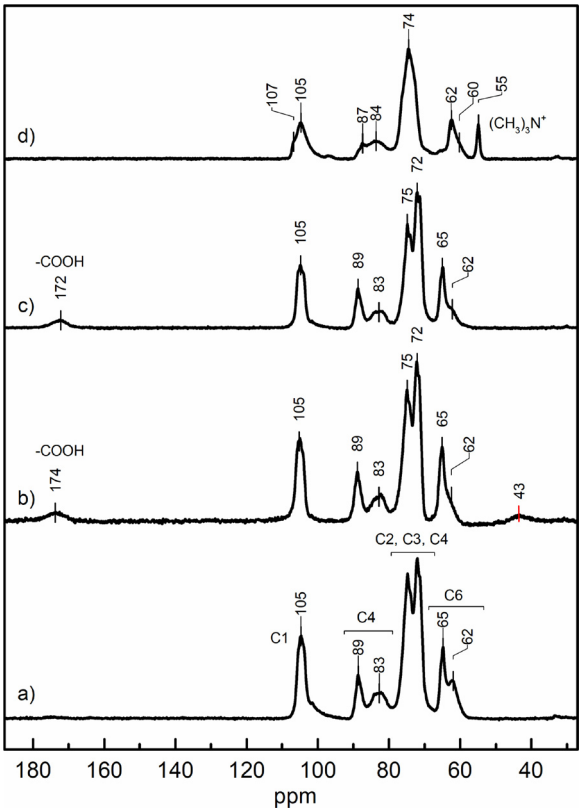

Fig. 5. NMR spectra for: a) CL, b) CLT, c) CLC, d) CLA.

in the peak at ~63 ppm corresponding to C-6 by a downfield chemical shift at 63 ppm. The phenomenon is probably due to the crosslinking process as a result of the reaction with citric acid anhydride, resulting in a more-ordered environment of CL chains (Atalla & VanderHart, 1999).

In Fig. 5d is shown the solid ^{13}C NMR spectrum of CLA, in which, when compared with the pre-treated CL, are seen new peaks, chemical shift variations, and band broadening of the peaks. The new peak at ~55 ppm is assigned to the ammonium quaternary group $(CH_3)_3N^+$ confirming that the reaction was accomplished. The chemical shifts in the region of 70–78 ppm are related to C-2, C-3, and C-5 of the pyranose ring. Also, in the region between 90-79 ppm related to C-4 has a smaller and wider peak than pre-treated CL as seen on Fig. 5a. In addition, an up-field of the chemical shift displacement of the region at 65-63 ppm assigned to C-6, is observed. However, the anomeric carbon (C-1) has a similar behaviour, although a small overlapped peak appears at 107 ppm. An explanation for the observed differences may be related to the presence of non-equivalent glycosidic linkages because of the harsh conditions (high temperature and a strong alkaline environment) that might produce a scission of the polymeric chain, thus generating a disintegration of the microfibrils. Furthermore, as depicted in FT-IR spectra (Fig. 2d), SEM analysis (Fig.4D) and ^{13}C NMR spectra (Fig. 5d) the degradation of CL microfibrils by the strong alkaline environment during the reaction can be noticed (Saini, Yucel Falco, Belgacem, & Bras, 2016), supporting this explanation.

3.3.5. FT-IR spectra of chemically modified CL

When CL, derived from the alkaline pre-treatment process (Fig. 6a) of SBH, reacts with citric acid anhydride, an esterification reaction occurs which is evident in Fig. 6b. The cellulosic hydroxyl groups form an ester linkage incorporating carboxylic acid groups into CL (Wayne E Marshall, Chatters, Wartelle, & McAloon, 2001; Wing, 1996). A strong characteristic stretching vibration band at 1717 cm^{-1} evidencing the functionalization of the CL, reflects the carboxyl groups. Similarly, an esterification reaction takes place when CL is treated with tartaric acid. As seen in Fig. 6c, a strong peak at 1734 cm^{-1} also appears revealing the result of tartaric acid esterification (Wong, Lee, Low, & Haron, 2003).

In order to obtain a cationic matrix by introducing positive charges

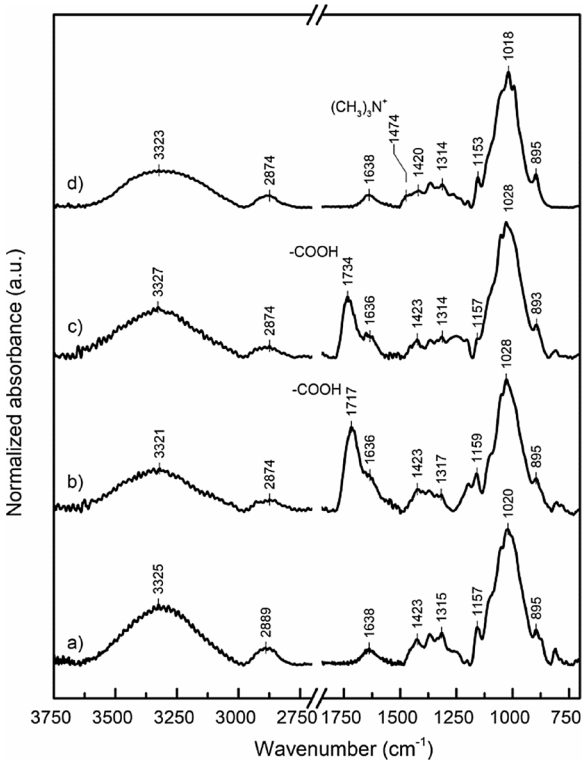

Fig. 6. FTIR spectra of: a) CL, b) CLC, c) CLT, d) CLA.

through the quaternization reaction, CL reacts with *N*-(3-chloro-2-hydroxypropyl) trimethylammonium chloride in the presence of a strong alkaline environment (Marshall & Wartelle, 2004).

Therefore, the presence of nitrogen in the matrix was detected by FT-IR spectra, C^{13} NMR and Kjeldahl analysis (data not shown). Fig. 6d does not show significant variations in comparison with the starting material, but a small broad peak associated with the stretching vibration of a C—N bond at 1474 cm^{-1} appears (Hu, Wang, Li, & Wang, 2014). However, in order to confirm the attachment of $(CH_3)_3N^+$, the same sample was analysed with ^{13}C-NMR technique, which showed a new peak at 55 ppm corresponding to the presence of quaternary ammonium group. C–N stretching vibrations from quaternary ammonium groups has a low signal intensity on FT-IR spectra. This may explain the difficulty of detecting this type of functional groups on Fig. 6d, which is consistent with the consulted bibliography (Anirudhan, Noeline, & Manohar, 2006; Hu et al., 2014).

On the other hand, the signal obtained in the region of 3400–3500 cm^{-1}, related to the stretching vibrations of the -OH groups present in the samples, decreases its intensity in the modified CL samples compared to the unmodified ones. This could be attributed to the decrease of -OH groups in the treated samples because they could be involved in the functionalization reactions.

Interesting to note that the spectra obtained confirms the conclusions performed in Section 3.2. The pre-treatment carried out on SBH allowed the obtention of the CL present in the biomass, eliminating the lignin present in it. This is evidenced by the absence of the characteristic peaks of lignin in the FT-IR, such as, for example, the peaks at 1239, 1540, 1641, and 1745 cm^{-1}.

3.3.6. The Raman spectroscopy measurements

Fig. 7 shows the Raman spectra of CL and CLA samples, where it can be seen the similarity of both Raman spectra, i.e, presenting modes in the same ranges (around 3000 and between 600 and 1600 cm^{-1}). However, the signature in the 3000 cm^{-1} range, assigned to C–H stretching vibrations, is less intense for CLA. Indeed, the intensity ratio between this band and the most intense one in the region of the C—C and C–O single bonds, i.e. 600-1600 cm^{-1} range (≈1091 cm^{-1} - the characteristic CL fingerprint) is 4.6 for CL sample and 1.8 for CLA sample, indicating a decrease in the number of C–H bounds in the CLA sample. Moreover, a more detailed analysis reveals that the corresponding modes for CLA are broader than for CL, revealing less crystallinity. However, as in the Raman spectrum of the CLA sample (as also on the CL) the 1157 cm^{-1} mode (present only in crystalline CL (Szymańska-Chargot, Cybulska, & Zdunek, 2011) is seen (inset of Fig. 7), it must be concluded that the CLA also has microcrystalline CL but highly disordered. Moreover, it is known that for this kind of material the presence of a peak around 913 cm^{-1}, is related to crystallinity, particularly to the crystallites size, and the broadening and shift of this mode to lower cm^{-1} indicates disorder, as observed for the CLA sample. According to (Schenzel & Fischer, 2004), the degree of crystallinity in cellulosic samples is related with the ratio of the intensity of the 1481 cm^{-1} mode by the sum of the intensity of 1481 cm^{-1} and 1462 cm^{-1} modes, which correspond to the CH_2 bending. However, typically these bands are less intense, as observed in the studied samples. Moreover, a more careful analysis at this range reveals that the CLA sample has a higher contribution of the 1462 cm^{-1} mode, which corresponds to the amorphous CL (inset of Fig. 7) when compared with the CL sample, confirming that CL corresponds to microcrystalline cellulose and CLA corresponds to a less crystalline cellulose. Indeed, the Raman spectra of CL sample, is very similar to the reported one of commercial microcrystalline CL (Szymańska-Chargot et al., 2011). Furthermore, the apparent decrease of the methine stretch at 2891 cm^{-1} in CLA is attributed to the loss of the CH_3 bonds. Finally, the near absence of the CL Raman modes in the Raman spectrum for CLC (not shown), indicates a strong degradation of the structural characteristic of CL, which may be due to the treatment with high temperature (125 °C). It is important to mention that for this sample a large background band, typically associated with luminescence, appears. This band can hide the CL Raman spectra and can appear due to the diffusion of ions (related with the process) to the surface, as observed with Fe (III) ions (Proniewicz et al., 2001). It is known (Agarwal, Reiner, & Ralph, 2010) by previous studies on pure CL that uses hydrothermal conditions, namely 100 °C result in less crystallinity and consequently loss of the Raman signal.

3.4. Thermogravimetry curves of CL and functionalized CL

Fig. 8a shows the comparative thermal behaviour of the pure CL and functionalized CL. Below 100 °C, a slight weight loss was observed for all the specimens. This is attributed to the vaporization of water, which is consistent with prior reports that state water interacts strongly by hydrogen bonds with the −OH groups of CL. The main thermal degradation stage occurred in the temperature range of 200–400 °C. A typical sigmoidal behaviour is observed in the curve residual mass vs. temperature, with an inflection point around 340 °C. The first derivate of these curves were obtained, such as shown in Fig. 8b, to determine the transition temperature and the number of transitions. Further heating until 500 °C revealed that the residual weight of the samples represented between 12 to 22% of the total initial mass. Lignin decomposes over a wide temperature range, from ambient to about 600 °C, with a very low mass loss rate, so the shape of the curves from Fig. 8a suggest that there is no lignin present in all the samples (Quan, Gao, & Song, 2016). These results agree with the FT-IR (Fig. 6) and NMR (Fig. 5) spectra of the samples obtained, where the distinctive peaks of lignocellulosic compounds are not found after the pre-treatment on the SBH was carried out. (Derkacheva & Sukhov, 2008; Xia, Akim, & Argyropoulos, 2001).

By observing the CL curve, it can be said that under argon atmosphere, CL decomposition was in a single step. This type of behaviour indicates that hemicelluloses and lignin were completely removed during the bleaching and pre-alkaline treatments. Considering that these last substances have different T_m compared to the CL, this

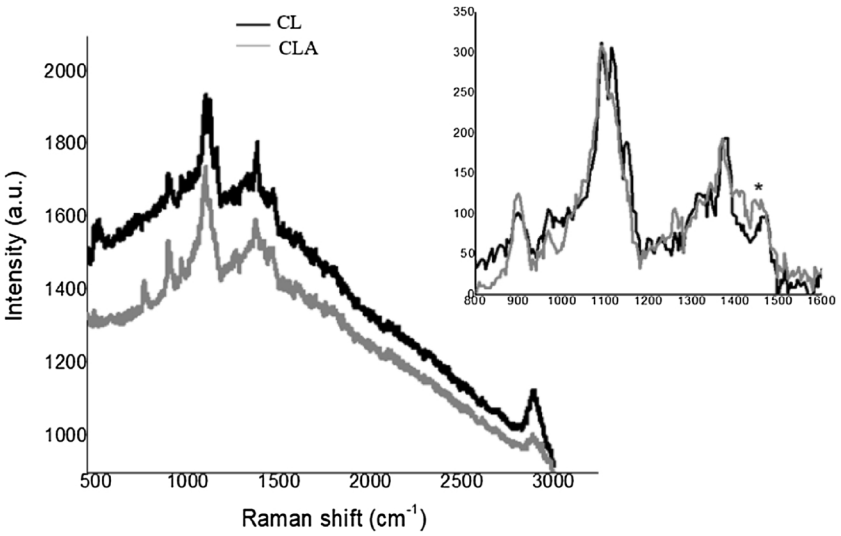

Fig. 7. Room temperature Raman spectra of CL and CLA.

confirms that the alkaline pre-treatment was effective by itself, which again confirms that this pre-treatment can effectively remove hemicelluloses and lignin. The maximum rate of decomposition of this CL occurred at 345 °C as determined by the maximum peak value. Variations in the temperature of maximum degradation rate of CL have been discussed in recent papers (Trache et al., 2014a,2014b); the shift of the T_m value may be influenced by the degree of crystallinity (Yang, Yan, Chen, Lee, & Zheng, 2007), by modification in the fibrillar structure of the CL due to a chemical treatment or due to the insertion of foreign chemical groups (Zhu et al., 2008). The first derivative curve for the CLA (see Fig. 8b) shows an anomalous behaviour by presenting two peaks, which suggested the presence of a heterogeneous CL structure compared to the fibrillar native CL.

Previous reports demonstrated that the thermal decomposition of CL could be divided into three main stages (Lee, Sundaram, Zhu, Zhao, & Mani, 2018; Teng, Yu, Fu, & Yin, 2018). Stage I occurs at a low temperature range, under 150 °C. Weight loss in this stage is mainly attributed to the evaporation of highly adsorbed water and volatile substances. As the temperature increases to approximately 200 °C, stage II, the inter- and intra-molecular hydrogen bonds rupture and water is generated. The molecular structure of CL is altered, and the polymerization degree of the CL chain decreases in a significant manner, promoting the production of char residue. Reactions such as dehydrogenation and decarbonization start to take place and intermediate active CL is produced (Szcześniak, Rachocki, & Tritt-Goc, 2007). Stage III is the main devolatilization phase where carbon and volatiles are released, and it takes place from 350 °C to 500 °C. Active CL is further decomposed and form levoglucosan and other oligosaccharides through transglucosidation (Wang, Yao, Zhou, & Zhang, 2017) which induces a high mass loss percentage found at this stage. The dTGA curves are symmetrical and there is only one sharp peak in each curve, indicating that a single stage thermal decomposition occurred during the pyrolysis of CL. The biphasic dTGA curves observed for CLA confirms that its decomposition is more complex and that the chemical products yielded from the thermal decomposition are different due to the presence of the amine group. The insertion of a chemical group into the CL structure induced a shift of the sigmoidal curves to the left, which confirms a smaller thermal stability of the material as shown. Table 1 shows the T_m values, where it is seen that CLC showed a slight decrease in the transition temperature T_m, about 20 °C, while CLT showed the presence of two peaks positioned at 250 °C and 325 °C, which suggested a different crosslinking mechanism with the polysaccharides chains compared to CLC (Zhu et al., 2008).

The thermal stability curve for CLA showed present two transitions, one with a T_m similar to the untreated CL and another with a minor peak around 292 °C. The N-(3-chloro-2-hydroxypropyl) trimethylammonium chloride introduces a quaternary ammonium group into the CL chains, then, as there is no possible interaction with polar groups of the polysaccharide a hydrogen bond cannot be formed, and this induces a decrease in the T_m value.

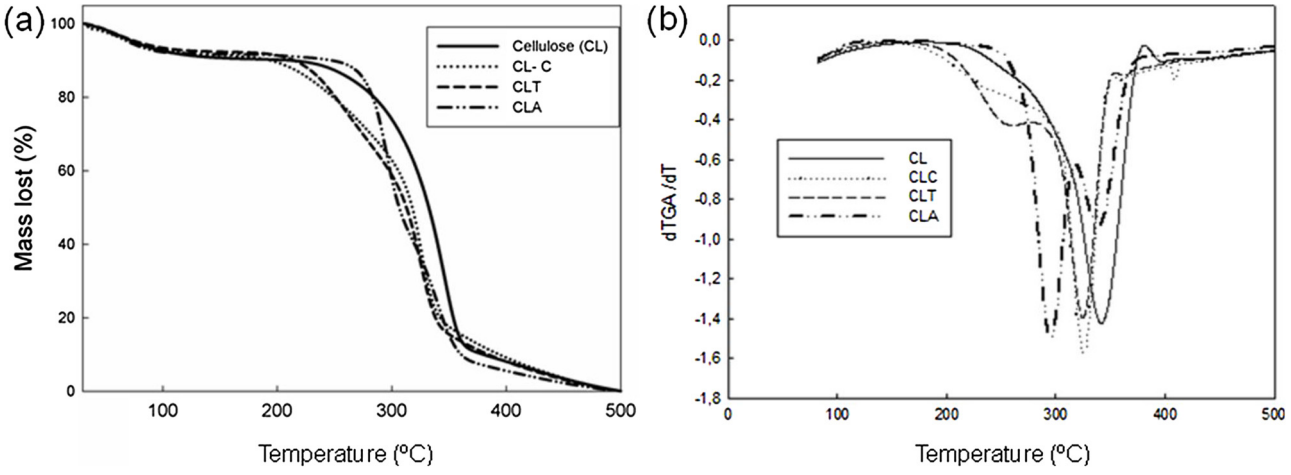

Fig. 8. a) TGA and b) derivative curves for the CL and functionalized CL. Heating rate: 5 grade /minute.

Table 2
Adsorption capacity of the CL and functionalized CL beds with model proteins. The results were expressed as a percentage (%) of bound protein.

Solute	CL	CLC	CLT	CLA
Lysozyme (pH 7.0)	100.0	89.5	70.9	–
Albumin (pH 7.0)	–	–	–	92.7

3.5. CL and functionalized CLs adsorption capacity for proteins

The adsorption capacity with two model proteins, lysozyme (pI 10.5) and albumin (pI 4.8) was assayed, to verify the feasibility of using the compounds obtained as adsorbent beds for bioseparation of enzymes in a scaled-up process. The assayed was carried in batch and the results found are shown in Table 2.

The adsorption of lysozyme was assayed onto CL, CLC and CLT. At pH 7.0, lysozyme has a positive electric charge, so CL showed to have a great capacity of protein adsorption due to the presence of negative electrical charge ($-COOH$); this was demonstrated in the acid base titration. CLT and CLC showed to also have a good capacity to adsorb lysozyme due to the multiples -COOH present in these beds. Albumins (pI around 4.8) at pH 7.0 did not show any adsorption onto CL, CLT and CLC, because this protein is negatively charge at this pH, while CLA showed a good capacity to adsorb it because it has a positive electrical charge due the strong quaternary ammonium groups.

4. Conclusions

In recent years more attention has been paid to sustainable, green and environmental friendly materials for various applications. In this work, a simple and mild method was assayed for the extraction of CL from lignocellulosic fibers of SBH.

SBH is a special waste due its low content of lignin (0.5 to 2.0% (w/w)) compared with other agriculture waste (15 to 20% w/w). Also, its three-dimensional structure is a lot more open, or permeable, respect to other residual waste such as wood, corn cab, rice hull, etc., so it is not necessary to apply the drastic standard methods used to extract CL from these biomass, such as sulfuric acid 65% combined with high temperature, where the final product must be neutralized, washed and unavoidably acid residues are discarded into the environment, ending up as pollution.

The slightly alkaline treatment for 40 h assayed in this work, successfully eliminated the lignocellulosic component in a safely, cost-efficient and complete manner. It was demonstrated by the absence of polyphenols in the CL, as seen on the FT-IR spectra (disappearance of the absorption peak at 1745 cm^{-1}) and confirmed by thermogravimetric analysis (TGA), where only one thermal transition is observed at 345 °C and which correspond to pure CL. On the other hand, because the amorphous CL has more polysaccharide chains exposed to the solvent, it is more prone to react with reagents that allow it to introduce -COOH or $(CH_3)_3N^+$ groups. The introduction of -COOH groups modified the physical qualities of the CL sample, obtaining a much more compact derivate, with a lower capacity of water absorption, due to the approach of the polysaccharide chains by crosslinking with carboxylic acids. On the contrary, the introduction of quaternary ammonium groups has a much less compact structure, which may be due to the high alkaline conditions that produces a disruption of CL microfibers. At the same time, SEM technique showed the presence of a more compact structure of the chemical derivatives with respect to the untreated CL, even when compared with the CL sample that has undergone a treatment with 20% (w/v) NaOH for several hours. This last one presents many opened fibers because the alkaline media has broken the intra polysaccharide hydrogen bridge in a way that favors the formation of a greater amorphous structure.

The modified CL obtained in this work showed good compaction capacity as well as a high capacity to retain macromolecules with an opposite electrical charge. That characteristics makes it an extremely effective ion exchanger. Furthermore, the cost of the CL extraction from the major Argentine agriculture waste is significantly lower (about 300$US/Tn) than that obtained from other sources, such as the case of wood (800$US/Tn). At the same time, this procedure has the advantage of inducing a low negative impact on the environment since only eco-friendly reagents were used and were capable to extract the lignocellulosic components to obtain CL. Besides all the above said, these final products could be used as beds in a scaled-up adsorption procedure for the purification of macromolecules of industrial interest.

Acknowledgements

This work was supported by grants from PICT-2013-271 and PICT-2015-0083 from FonCyT, Ministerio de Ciencia, Tecnología e Innovación Productiva de Argentina. MEB and PC are fellowship from Agencia.

References

Agarwal, U. P., Reiner, R. S., & Ralph, S. A. (2010). Cellulose I crystallinity determination using FT–Raman spectroscopy: Univariate and multivariate methods. *Cellulose, 17*(4), 721–733.

Ahuja, D., Kaushik, A., & Singh, M. (2018). Simultaneous extraction of lignin and cellulose nanofibrils from waste jute bags using one pot pre-treatment. *International Journal of Biological Macromolecules, 107*(Pt A), 1294–1301. https://doi.org/10.1016/j.ijbiomac.2017.09.107.

Andrade-Mahecha, M. M., Pelissari, F. M., Tapia-Blacido, D. R., & Menegalli, F. C. (2015). Achira as a source of biodegradable materials: Isolation and characterization of nanofibers. *Carbohydrate Polymers, 123*, 406–415. https://doi.org/10.1016/j.carbpol.2015.01.027.

Anirudhan, T. S., Noeline, B., & Manohar, D. (2006). Phosphate removal from wastewaters using a weak anion exchanger prepared from a lignocellulosic residue. *Environmental Science & Technology, 40*(8), 2740–2745.

Atalla, R., & VanderHart, D. L. (1999). The role of solid state 13C NMR spectroscopy in studies of the nature of native celluloses. *Solid State Nuclear Magnetic Resonance, 15*(1), 1–19.

Carvajal, J. C., Gomez, A., & Cardona, C. A. (2016). Comparison of lignin extraction processes: Economic and environmental assessment. *Bioresource Technology, 214*, 468–476. https://doi.org/10.1016/j.biortech.2016.04.103.

Chen, L., Zhu, J. Y., Baez, C., Kitin, P., & Elder, T. (2016). Highly thermal-stable and functional cellulose nanocrystals and nanofibrils produced using fully recyclable organic acids. *Green Chemistry, 18*(13), 3835–3843. https://doi.org/10.1039/c6gc00687f.

Chukwuemeka, P., Azubuike, J. O. O., Augustine, O., & Okhamafec (2012). Physicotechnical, spectroscopic and thermogravimetric properties of powdered cellulose and microcrystalline cellulose derived from groundnut shells. *Journal of Excipients and Food Chemicals, 3*(3), 106–115.

Derkacheva, O., & Sukhov, D. (2008). *Investigation of lignins by FTIR spectroscopy. Paper presented at the macromolecular symposia.*

Eberts, T. J., Sample, R., Glick, M., & Ellis, G. (1979). A simplified, colorimetric micromethod for xylose in serum or urine, with phloroglucinol. *Clinical Chemistry, 25*(8), 1440–1443.

Ferrer, A., Salas, C., & Rojas, O. J. (2016). Physical, thermal, chemical and rheological characterization of cellulosic microfibrils and microparticles produced from soybean hulls. *Industrial Crops and Products, 84*, 337–343. https://doi.org/10.1016/j.indcrop.2016.02.014.

Fiol, N., & Villaescusa, I. (2009). Determination of sorbent point zero charge: Usefulness in sorption studies. *Environmental Chemistry Letters, 7*(1), 79–84.

Flauzino Neto, W. P., Silvério, H. A., Dantas, N. O., & Pasquini, D. (2013). Extraction and characterization of cellulose nanocrystals from agro-industrial residue – Soy hulls. *Industrial Crops and Products, 42*, 480–488. https://doi.org/10.1016/j.indcrop.2012.06.041.

González, M., Guzmán, B., Rudyk, R., Romano, E., & Molina, M. A. (2003). Spectrophotometric determination of phenolic compounds in propolis. *Acta Farmaceutica Bonaerense, 22*(3), 243–248.

Horn, S. J., Vaaje-Kolstad, G., Westereng, B., & Eijsink, V. (2012). Novel enzymes for the degradation of cellulose. *Biotechnology for Biofuels, 5*(1), 45.

Hu, D., Wang, P., Li, J., & Wang, L. (2014). Functionalization of microcrystalline cellulose with n, n-dimethyldodecylamine for the removal of congo red dye from an aqueous solution. *Bioresources, 9*(4), 5951–5962.

Karki, B., Maurer, D., & Jung, S. (2011). Efficiency of pretreatments for optimal enzymatic saccharification of soybean fiber. *Bioresource Technology, 102*(11), 6522–6528. https://doi.org/10.1016/j.biortech.2011.03.014.

Kim, S. H., Lee, C. M., & Kafle, K. (2013). Characterization of crystalline cellulose in biomass: Basic principles, applications, and limitations of XRD, NMR, IR, Raman, and SFG. *Korean Journal of Chemical Engineering, 30*(12), 2127–2141. https://doi.org/10.1007/s11814-013-0162-0.

Kirk, T. K., & Obst, J. R. (1988). *Lignin determination methods in enzymology, Vol. 161*, Elsevier87–101.
Kumar, H., & Christopher, L. P. (2017). Recent trends and developments in dissolving pulp production and application. *Cellulose, 24*(6), 2347–2365. https://doi.org/10.1007/s10570-017-1285-y.
Lee, H., Sundaram, J., Zhu, L., Zhao, Y., & Mani, S. (2018). Improved thermal stability of cellulose nanofibrils using low-concentration alkaline pretreatment. *Carbohydrate Polymers, 181*, 506–513. https://doi.org/10.1016/j.carbpol.2017.08.119.
Liu, H. M., Wang, F. Y., & Liu, Y. L. (2016). Hot-compressed water extraction of polysaccharides from soy hulls. *Food Chemistry, 202*, 104–109. https://doi.org/10.1016/j.foodchem.2016.01.129.
Lu, P., & Hsieh, Y.-L. (2010). Preparation and properties of cellulose nanocrystals: Rods, spheres, and network. *Carbohydrate Polymers, 82*(2), 329–336. https://doi.org/10.1016/j.carbpol.2010.04.073.
Marsden, W. L., Gray, P. P., Nippard, G. J., & Quinlan, M. R. (1982). Evaluation of the DNS method for analysing lignocellulosic hydrolysates. *Journal of Chemical Technology and Biotechnology, 32*(7–12), 1016–1022.
Marshall, W. E., & Wartelle, L. H. (2004). An anion exchange resin from soybean hulls. *Journal of Chemical Technology & Biotechnology, 79*(11), 1286–1292. https://doi.org/10.1002/jctb.1126.
Marshall, W. E., Chatters, A. Z., Wartelle, L. H., & McAloon, A. (2001). Optimization and estimated production cost of a citric acid-modified soybean hull ion exchanger. *Industrial Crops and Products, 14*(3), 191–199.
Marshall, W. E., Wartelle, L., Boler, D., Johns, M., & Toles, C. (1999). Enhanced metal adsorption by soybean hulls modified with citric acid. *Bioresource Technology, 69*(3), 263–268.
Martelli-Tosi, M., Torricillas, M.d. S., Martins, M. A., Assis, O. B. G.d., & Tapia-Blácido, D. R. (2016). Using commercial enzymes to produce cellulose nanofibers from soybean straw. *Journal of Nanomaterials, 2016*, 1–10. https://doi.org/10.1155/2016/8106814.
McIntosh, S., & Vancov, T. (2011). Optimisation of dilute alkaline pretreatment for enzymatic saccharification of wheat straw. *Biomass and Bioenergy, 35*(7), 3094–3103.
Mendoza, A. J. (2014). Tartaric acid cross-linking of starch: Effects of reaction conditions on the maximum tensile strength of cast plastic films. *Canadian Young Scientist Journal, 2015*(1), 1–9.
Ng, H.-M., Sin, L. T., Tee, T.-T., Bee, S.-T., Hui, D., Low, C.-Y., ... Rahmat, A. R. (2015). Extraction of cellulose nanocrystals from plant sources for application as reinforcing agent in polymers. *Composites Part B: Engineering, 75*, 176–200. https://doi.org/10.1016/j.compositesb.2015.01.008.
Oh, S. Y., Yoo, D. I., Shin, Y., Kim, H. C., Kim, H. Y., Chung, Y. S., ... Youk, J. H. (2005). Crystalline structure analysis of cellulose treated with sodium hydroxide and carbon dioxide by means of X-ray diffraction and FTIR spectroscopy. *Carbohydrate Research, 340*(15), 2376–2391. https://doi.org/10.1016/j.carres.2005.08.007.
Pandey, K. (1999). A study of chemical structure of soft and hardwood and wood polymers by FTIR spectroscopy. *Journal of Applied Polymer Science, 71*(12), 1969–1975.
Phinichka, N., & Kaenthong, S. (2018). Regenerated cellulose from high alpha cellulose pulp of steam-exploded sugarcane bagasse. *Journal of Materials Research and Technology, 7*(1), 55–65. https://doi.org/10.1016/j.jmrt.2017.04.003.
Prado, H. J., & Matulewicz, M. C. (2014). Cationization of polysaccharides: A path to greener derivatives with many industrial applications. *European Polymer Journal, 52*, 53–75. https://doi.org/10.1016/j.eurpolymj.2013.12.011.
Proniewicz, L. M., Paluszkiewicz, C., Wesełucha-Birczyńska, A., Majcherczyk, H., Barański, A., & Konieczna, A. (2001). FT-IR and FT-Raman study of hydrothermally degradated cellulose. *Journal of Molecular Structure, 596*(1-3), 163–169.
Quan, C., Gao, N., & Song, Q. (2016). Pyrolysis of biomass components in a TGA and a fixed-bed reactor: Thermochemical behaviors, kinetics, and product characterization. *Journal of Analytical and Applied Pyrolysis, 121*, 84–92. https://doi.org/10.1016/j.jaap.2016.07.005.
Saini, S., Yucel Falco, C., Belgacem, M. N., & Bras, J. (2016). Surface cationized cellulose nanofibrils for the production of contact active antimicrobial surfaces. *Carbohydrate Polymers, 135*, 239–247. https://doi.org/10.1016/j.carbpol.2015.09.002.
Salis, A., Bostrom, M., Medda, L., Cugia, F., Barse, B., Parsons, D. F., ... Monduzzi, M. (2011). Measurements and theoretical interpretation of points of zero charge/potential of BSA protein. *Langmuir, 27*(18), 11597–11604. https://doi.org/10.1021/la2024605.
Schenzel, K., & Fischer, S. (2004). Applications of FT raman spectroscopy for the characterization of cellulose. *Biomaterials, 1*, 9.
Stefanidis, S. D., Kalogiannis, K. G., Iliopoulou, E. F., Michailof, C. M., Pilavachi, P. A., & Lappas, A. A. (2014). A study of lignocellulosic biomass pyrolysis via the pyrolysis of cellulose, hemicellulose and lignin. *Journal of Analytical and Applied Pyrolysis, 105*, 143–150. https://doi.org/10.1016/j.jaap.2013.10.013.
Sun, X. F., Xu, F., Sun, R. C., Fowler, P., & Baird, M. S. (2005). Characteristics of degraded cellulose obtained from steam-exploded wheat straw. *Carbohydrate Research, 340*(1), 97–106. https://doi.org/10.1016/j.carres.2004.10.022.
Szcześniak, L., Rachocki, A., & Tritt-Goc, J. (2007). Glass transition temperature and thermal decomposition of cellulose powder. *Cellulose, 15*(3), 445–451. https://doi.org/10.1007/s10570-007-9192-2.
Szymańska-Chargot, M., Cybulska, J., & Zdunek, A. (2011). Sensing the structural differences in cellulose from apple and bacterial cell wall materials by Raman and FT-IR spectroscopy. *Sensors, 11*(6), 5543–5560.
Teng, Y., Yu, G., Fu, Y., & Yin, C. (2018). The preparation and study of regenerated cellulose fibers by cellulose carbamate pathway. *International Journal of Biological Macromolecules, 107*(Pt A), 383–392. https://doi.org/10.1016/j.ijbiomac.2017.09.006.
Trache, D., Hussin, M. H., Hui Chuin, C. T., Sabar, S., Fazita, M. R., Taiwo, O. F., ... Haafiz, M. K. (2016). Microcrystalline cellulose: Isolation, characterization and bio-composites application-a review. *International Journal of Biological Macromolecules, 93*(Pt A), 789–804. https://doi.org/10.1016/j.ijbiomac.2016.09.056.
Trache, D., Donnot, A., Khimeche, K., Benelmir, R., & Brosse, N. (2014a). Physico-chemical properties and thermal stability of microcrystalline cellulose isolated from Alfa fibres. *Carbohydrate Polymers, 104*, 223–230.
Trache, D., Donnot, A., Khimeche, K., Benelmir, R., & Brosse, N. (2014b). Physico-chemical properties and thermal stability of microcrystalline cellulose isolated from Alfa fibres. *Carbohydrate Polymers, 104*, 223–230. https://doi.org/10.1016/j.carbpol.2014.01.058.
Tsuboi, M. (1957). Infrared spectrum and crystal structure of cellulose. *Journal of Polymer Science Part A: Polymer Chemistry, 25*(109), 159–171.
Van Soest, P., Horvath, P., McBurney, M., Jeraci, J., & Allen, M. (1983). *Some in vitro and in vivo properties of dietary fibers from noncereal sources.* ACS Publications.
Wang, Z., Yao, Z., Zhou, J., & Zhang, Y. (2017). Reuse of waste cotton cloth for the extraction of cellulose nanocrystals. *Carbohydrate Polymers, 157*, 945–952. https://doi.org/10.1016/j.carbpol.2016.10.044.
Wing, R. E. (1996). Starch citrate: Preparation and ion exchange properties. *Starch–Stärke, 48*(7–8), 275–279.
Wong, K., Lee, C., Low, K., & Haron, M. (2003). Removal of Cu and Pb by tartaric acid modified rice husk from aqueous solutions. *Chemosphere, 50*(1), 23–28.
Xia, Z., Akim, L. G., & Argyropoulos, D. S. (2001). Quantitative 13C NMR analysis of lignins with internal standards. *Journal of Agricultural and Food Chemistry, 49*(8), 3573–3578.
Xiao, B., Sun, X., & Sun, R. (2001). Chemical, structural, and thermal characterizations of alkali-soluble lignins and hemicelluloses, and cellulose from maize stems, rye straw, and rice straw. *Polymer Degradation and Stability, 74*(2), 307–319.
Yang, H., Yan, R., Chen, H., Lee, D. H., & Zheng, C. (2007). Characteristics of hemicellulose, cellulose and lignin pyrolysis. *Fuel, 86*(12–13), 1781–1788. https://doi.org/10.1016/j.fuel.2006.12.013.
Yeo, J. Y., Chin, B. L. F., Tan, J. K., & Loh, Y. S. (2017). Comparative studies on the pyrolysis of cellulose, hemicellulose, and lignin based on combined kinetics. *Journal of the Energy Institute*. https://doi.org/10.1016/j.joei.2017.12.003.
Zhu, B., Fan, T., & Zhang, D. (2008). Adsorption of copper ions from aqueous solution by citric acid modified soybean straw. *Journal of Hazardous Materials, 153*(1-2), 300–308. https://doi.org/10.1016/j.jhazmat.2007.08.050.